

Scale Separation for Moisture-laden Regions in the Tropical Atmosphere

G. Bellon, M. Ghil¹, and H. Le Treut

Laboratoire de Météorologie Dynamique du CNRS, Institut Pierre-Simon Laplace, Ecole Normale Supérieure, Paris, France.

The size distribution of moist regions in the tropical atmosphere exhibits two modes of organization, one at synoptic scales and the other at planetary scales. We show the existence of these two modes in two data sets: column-integrated precipitable water and outgoing long-wave radiation. A simple two-column model of radiation and convection in the Tropics helps interpret the presence of these two modes. The coupling between radiative effects and low-level atmospheric dynamics provides a plausible mechanism for scale selection.

1. Introduction

It is well known by now that tropospheric water vapor in the Tropics is bimodal [*Pierrehumbert, 1995*]: the observed distribution of upper-tropospheric humidity exhibits a moist mode near 75% and a dry mode near 20%. This bimodality arises from rate differences in the processes that control the vertical and horizontal transport of water vapor [*Zhang et al., 2003*]. The injection of water vapor into the free troposphere by deep convection is very fast (a few hours) and is responsible for the moist mode. Radiatively driven subsidence gives rise to the dry mode. This mode is maintained against horizontal mixing, which acts to homogenize the humidity distribution, provided the subsidence time scale is shorter than that of the mixing. The purpose of the present paper is to study the scale distribution of the moist patches.

The bimodality of the humidity distribution can be detected in data sets with mesoscale definition in space (up to 10^2 km) and time (3 h to 1 day), as well as in data sets with climatological definition in space (10^3 km) and time (1 month) [*Zhang et al., 2003*]. The present paper investigates the spatial scales that characterize this bimodal distribution.

A radiative-convective box model of the tropical atmosphere that features an ascending moist column and a subsiding dry column [*Pierrehumbert, 1995; Larson et al., 1999; Bellon et al., 2003*] was originally formulated to capture key features of the Hadley and Walker circulations on long time scales. New data sets suggest that this type of model can represent the same bimodality on the mesoscale in space and scales of about a day in time. The circulation between the two columns is similar at the planetary and mesoscale: air in the moist convective regions ascends on average, the relatively dry air detrained at high altitude from the clouds descends throughout the surrounding clear-sky regions, and the low-level flow returns boundary-layer air to the moist convective regions. An important limitation of this conceptual model is its steady-state character. Still, tropical convection is organized into mesoscale clusters that are in

quasi-equilibrium with the large-scale forcing [*Arakawa and Schubert, 1974*].

The water vapor feedback is the main positive feedback on perturbations of the tropical climate and is often studied using a single-column model [*Held and Soden, 2000*]. Investigating the processes that control the extent of moist regions and their interaction with their subsiding counterparts goes one step beyond such models. How convection is spatially organized and how convective and subsiding structures interact in the atmosphere are thus important issues in unravelling the factors that control the tropical climate. These processes are expected to depend on the horizontal scale of the two-column, moist-vs.-dry system. We focus here on the observed size distribution and spectral properties of the moist structures, and propose a simple model to help explain these properties.

2. Size Distribution of Observed Convective Regions

2.1. Data and Methodology

We use two data sets to define the state of the tropical atmosphere: column-integrated precipitable water (PW) and outgoing longwave radiation (OLR). The first dataset is taken from the European Centre for Medium-Range Weather Forecast reanalysis project ERA40 [*Simmons and Gibson, 2000*], with a resolution of $1.125^\circ \times 1.125^\circ$, four times a day. The second set is daily data from the National Oceanic and Atmospheric Administration [*Liebmann and Smith, 1996*], with a spatial resolution of $2.5^\circ \times 2.5^\circ$. We limit our analysis to the Tropics (30°S – 30°N), and we use 24 years of the two data sets (1979–2002). While the precipitable water data contain information exclusively about the water content of the atmosphere, the OLR data set represents more complex signals: it contains information about the surface temperature and the temperature profiles, as well as the cloudiness and type of clouds in the column. Nevertheless, small OLR values are well correlated with moist atmospheric columns in the Tropics.

We computed the size distribution of the moist structures. For a given threshold of PW or OLR, a moist structure is defined as a connected set of gridpoints that are moister than the threshold, i.e., that have a larger value of PW or a lower OLR. The segmentation technique we use to determine these connected sets is Connected Component Labeling [*Rosenfeld and Kak, 1982*], which is based on a quad-tree data structure and neighbor-finding techniques [*Samet, 1989*]. The characteristic size of a moist region is given by the radius of the circle of same area, independently of the shape of the region.

We focus on the long-term mean distribution: for each day, the number and size of the moist regions is computed and the results are cumulated over the 24-yr period of the data sets (1979–2002). Each moist structure thus contributes in proportion to the length of its life span.

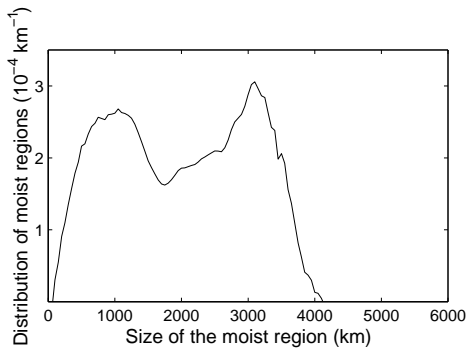


Figure 1. Distribution of the contribution to the total moist area as a function of the characteristic size of the moist region, using a threshold of PW (50 kg m^{-2}). The linear characteristic scale of a region is defined as the radius of a circular disk of the same area.

2.2. Observational results

Figure 1 shows the contribution of moist structures of a given size to the total area covered by the moist atmosphere for a threshold of PW = 50 kg m^{-2} . The distribution of the total moist area exhibits two modes: one for synoptic-scale structures that correspond to the size of convective clusters and superclusters, the other that corresponds to the large-scale signature of the Intertropical Convergence Zone and the Hadley and Walker circulations. The two modes are separated by a broad minimum in the distribution at sizes around 2000 km.

The distribution in Fig. 1 may be sensitive to the chosen threshold. Figure 2a shows the cumulated contribution of moist structures as a function of their size and the chosen threshold. For a very high threshold, only small structures

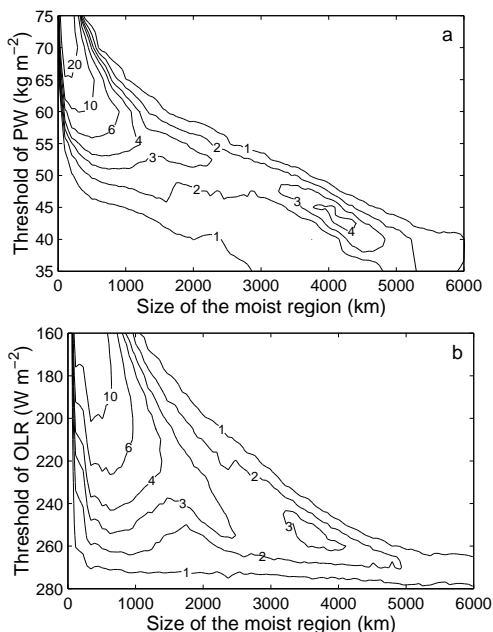


Figure 2. Distribution of the contribution to the total moist area (in 10^{-4} km^{-1}) as a function of the characteristic size of the moist region and the discriminating threshold. The threshold is based on (a) PW and (b) OLR.

are diagnosed as being humid: they are regions of intense convection organized on the mesoscale and synoptic scale. The second mode appears for thresholds about 50 kg m^{-2} and for characteristic sizes of about 3500 km. The large structures arise by the large-scale organization of smaller-scale, high-moisture structures that are connected by regions of moderate humidity; the latter are still moister than subsident regions, whose precipitable water is typically as low as 30 kg m^{-2} and lower. These large structures are actually the signature of the ascending branches of the Hadley and Walker circulations in the daily data.

Figure 2b shows analogous results when using the OLR data sets. The size distribution exhibits one mode at synoptic scales and a second, large-scale one. The amplitude and size range of the latter mode are smaller in this data set than in the PW data. This comparison shows that — given a large-scale humid structure, as determined by precipitable water — only the central part of its area radiates weakly to space: very deep convection occurs only in this part, while the convection in the remaining area of the structure is less intense.

In both data sets, the synoptic-scale mode exhibits a fork around 1500 km. Since this fork is more pronounced in the OLR data set, it seems to be associated with cirrus clouds issuing from the convective anvils that generate them. These high clouds have a strong signature in the OLR data because of their low temperature, while their water content is relatively small and their signal in the precipitable water data is, therefore, weaker.

3. A Two-Column Model with Dynamics

To investigate the reasons for the scale separation, we use a two-column radiative-convective model (RCM) developed by *Bellon et al.* [2003] and add to it a closure on the convection [*Larson et al.*, 1999]. This RCM belongs to the family of models initiated by *Pierrehumbert* [1995] that feature a convective and a subsiding column. Each column contains three boxes: free atmosphere, planetary boundary layer, and ocean mixed layer. No horizontal scale is specified for the two-column system, but the two columns may cover unequal areas. The two columns exhibit the same temperature profile in the free troposphere, but different relative humidities, in order to represent the observed bimodality of humidity. In the convective column, the boundary layer thermodynamic variables are coupled to the free-tropospheric values by deep convection.

The prognostic variables of our model are: (i) the temperatures in the free troposphere, in the boundary layer of the subsiding column, and in the two oceanic boxes; (ii) the free-tropospheric relative humidities in each column and the specific humidity in the boundary layer of the subsiding column; and (iii) the depth of this boundary layer. The circulation between the two columns is constrained by the energy balance of the dry free troposphere, where the warming by subsidence compensates the radiative cooling. Consequently, the large-scale circulation depends on the size of the subsiding column relative to the size of the convective column, but it is independent of the horizontal extent of the combined two-column system.

The radiatively constrained vertical circulation is associated with the divergence of the horizontal flow. This divergence is in turn related to horizontal pressure gradients, and it is thus expected to depend on the horizontal extent of the two-column system. Therefore, the adjustment between the vertical and horizontal circulations could act as a scale selection mechanism. We illustrate this idea by introducing a simple parameterization of the near-surface dynamics in

our RCM and analyzing the horizontal scales that can be represented by the modified model.

3.1. Dimensional analysis of the surface dynamics

Our surface-dynamics model is based on a reduced-gravity, shallow-water model [Gill, 1980; Lindzen and Nigam, 1987; Battisti et al., 1999]. It features a well-mixed boundary layer of constant virtual potential temperature that is tied to the sea surface temperature (SST) by the turbulent fluxes, and is topped by an infinitely thin inversion layer represented by a fixed jump ΔT_{inv} in temperature. The depth of the boundary layer is variable. The low-level winds represent perturbations from a reference state of rest with a given SST and depth of the boundary layer. They are forced by the horizontal variations of the pressure that result from the gradients of virtual potential temperature.

In this model, the linear momentum equation is:

$$\epsilon \mathbf{u} + f \mathbf{k} \times \mathbf{u} = -\nabla \Phi, \quad (1)$$

where \mathbf{u} is the mass-weighted average boundary-layer horizontal velocity, f the local Coriolis parameter, \mathbf{k} a unit vector in the vertical, and ϵ a surface drag coefficient. In the Tropics, mechanical damping is observed to happen on a time scale of one to two days, i.e., $\epsilon^{-1} = 1-2$ days. Stevens et al. [2002] have shown that another term, due to entrainment of free-tropospheric air into the boundary layer, should be added. Nevertheless, in our two-column framework, the free-tropospheric wind is the return flow from the low-level wind, and can therefore be considered as proportional to the boundary-layer wind. In this case, the effect of entrainment can be included by modifying slightly the parameter ϵ .

An analytical expression for the wind \mathbf{u} can be obtained from Equation (1). On a β -plane, the variation of the Coriolis parameter with latitude y , $f = f_0 + \beta y$, introduces a dependence of the divergence $\nabla \cdot \mathbf{u}$ on the pressure gradient $\nabla \Phi$:

$$\begin{aligned} \nabla \cdot \mathbf{u} = & -\frac{\epsilon}{\epsilon^2 + f^2} \nabla^2 \Phi \\ & + \frac{\beta \mathbf{j}}{(\epsilon^2 + f^2)^2} \cdot [2\epsilon f \nabla \Phi + (\epsilon^2 - f^2) \mathbf{k} \times \nabla \Phi]. \quad (2) \end{aligned}$$

The first term on the right-hand side of Equation (2) is proportional to the Laplacian of Φ , while the second term, called ‘‘Beta divergence’’ [Lindzen and Nigam, 1987], is proportional to the gradient of Φ . The competition between these two terms is a potential mechanism for the selection of horizontal scales.

To examine this possibility, we have carried out a dimensional analysis of Equation (2) in terms of the characteristic horizontal variation of Φ and the horizontal extent R of the two-column system described by the model. In this analysis, we applied two preliminary assumptions involving the geometries of the moist structure and pressure field: (i) the first-order terms proportional to β that are due to the variations of $\epsilon^2 + f^2$ and independent of the gradient in Φ are negligible with respect to the terms that are proportional to this gradient; and (ii) the second-order terms in β are negligible compared to the zero- and first-order terms. Applying these assumptions, our analysis shows that the Beta-divergence term is linear in the inverse horizontal scale R^{-1} , while the Laplacian term is quadratic in it. This balance between a linear and a quadratic term in R^{-1} leads to the existence of two characteristic scales.

To determine more quantitatively these two scales requires a parameterization of the surface dynamics in our RCM. We can express the average boundary-layer divergence $\overline{\nabla \cdot \mathbf{u}}$ in the subsiding column as

$$\overline{\nabla \cdot \mathbf{u}} = -\mu \left(\frac{\Delta \Phi}{R^2} - k \frac{\Delta \Phi}{R} \right); \quad (3)$$

$\Delta \Phi$ here is the boundary-layer pressure difference between the RCM’s convective column and the subsiding one. There are two parameters in Equation (3): μ is a mixed friction–Coriolis coefficient, while k accounts for the β effect; μ is of the order of a week (with $\epsilon^{-1} = 1$ day, $\mu = 6.5$ days at the Equator for a sinusoidal temperature perturbation) and $|k|$ of the order of $10^{-7} - 10^{-6} \text{ m}^{-1}$.

For a given thermodynamical state of the two-column model, Equation (3) is quadratic in R^{-1} . We can thus expect the model to have two equilibria, with two distinct scales R . Furthermore, since the warming by subsidence has to compensate the radiative cooling, the circulation between the two columns cannot physically be zero at equilibrium and thus $\overline{\nabla \cdot \mathbf{u}} \neq 0$. It follows from Equation (3) that the model cannot, therefore, represent a two-column system of horizontal extent $R = 1/k$, and a scale separation can thus be expected. Note that the existence of this scale separation is, in fact, independent of the parameterization of Φ .

3.2. Model results

For the sake of definiteness, we use here the parameterization of the perturbation of the vertically averaged pressure Φ introduced by Battisti et al. [1999]; this perturbation is parameterized as the sum of a term due to the SST variations and another term proportional to the wind divergence $\nabla \cdot \mathbf{u}$, called the ‘‘back pressure’’ [Lindzen and Nigam, 1987]:

$$\Phi = -\Gamma T'_s - c^2 / \epsilon (1 - \beta') \nabla \cdot \mathbf{u}; \quad (4)$$

here c is the atmospheric wave speed and β' accounts for the effect of convection: $\beta' = 1 - \epsilon \epsilon_m^{-1}$ if convecting, while

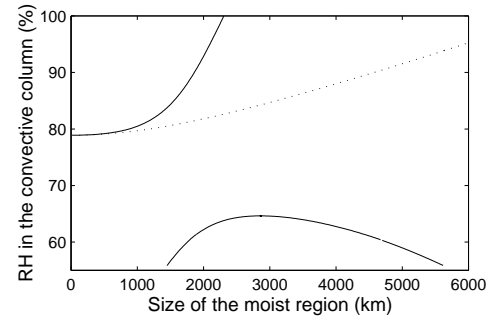


Figure 3. Relative humidity RH in the model’s convective column as a function of its horizontal scale R_c ; solid curve: case $(\mu, k) = (8 \text{ days}, 3.10^{-7} \text{ m}^{-1})$; dotted curve: same with $k = 0$.

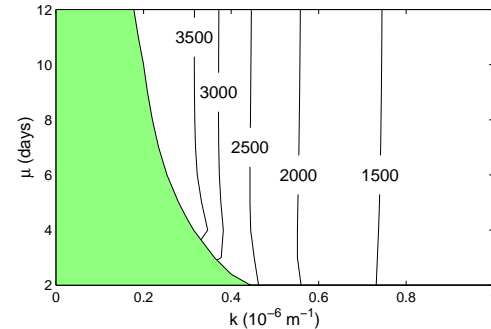


Figure 4. Sensitivity of the characteristic scale (in km) separating the two modes in the model; shaded: values of the parameters for which the model is unimodal.

$\beta' = 0$ otherwise. We use the values $\epsilon_m^{-1} = 6$ hours, $\Gamma = 50 \text{ m}^2\text{s}^{-2}\text{K}^{-1}$ and $c = 18 \text{ ms}^{-1}$.

Model results as a function of its horizontal scale R are reported here for $\epsilon^{-1} = 1$ day. Figure 3 shows the model relative humidity in the moist column as a function of its horizontal extent $R_c = A_c^{1/2}R$, where A_c is the relative area covered by the convective column. Two distinct modes can be seen: a very moist synoptic-scale one, and a dryer large-scale one. This pattern is very similar to the observations shown in Figs. 1 and 2, though the simple model's relative humidity is large compared to the observed upper-tropospheric values in Fig. 2a. In spite of this quantitative discrepancy, the highly idealized model appears to explain the two observed modes in the size distribution of the moist regions.

In the absence of Beta convergence ($k = 0$), the model exhibits only the synoptic-scale mode, which extends in this case to larger scales (see dotted line in Fig. 3). This single equilibrium is also characterized by a relative humidity that is higher than expected for a large-scale moist region.

The parameters μ and k are not very well constrained. We thus study the sensitivity of our results to changes of these parameters. Figure 4 shows the characteristic size of the separation between the synoptic-scale and large-scale modes, as a function of μ and k . This characteristic size is not very sensitive to changes in μ , as can be expected from the formulation of Equation (3). The two modes coexist for an extended range of parameters, for $k > 2 \cdot 10^{-7} \text{ m}^{-1}$. The characteristic scale that separates the two modes is of the observed order of magnitude, around 2000 km, for a large range of parameters as well.

4. Discussion

The existence of two modes in the observed daily distribution of the tropical moist structures is a remarkable feature. The convection associated with the planetary-scale Hadley and Walker circulations is thus not only a time-average characteristic of the Tropics, but can be seen in daily data as well. The scale separation suggests, furthermore, that convection and moistening of the atmosphere are organized differently on the planetary and the synoptic scale. The two modes are characterized by different ranges of humidity: the synoptic-scale mode is very moist, while the large-scale structures are less humid.

Our observational results are in fair agreement with the two equilibria of a simple two-column model. The model parameterizes the surface flow between the two columns using a dimensional analysis of the linear momentum equation. The existence of two separate modes, with distinct spatial scales, in the model relies on including near-surface-flow dynamics in the original thermodynamic model. The spatial scales are selected by the competition between the model's two divergence terms. While the Laplacian term is exclusively driven by the SST forcing, the Beta-divergence term is due to the variation of the Coriolis parameter with latitude; the inclusion of the latter is necessary to the existence of the large-scale mode. These model results are valid in an extended range of parameters.

To conclude, the existence of scale separation in the size distribution of moist structures — as found in observations and explained by our simple model — raises doubts about approaches that consider convection to be organized in the

same way on different space scales. In these approaches, convective structures are viewed as self-similar, fractal or multifractal [Lovejoy, 1982; Cahalan and Joseph, 1988]. Based so far on cloud data that do not exhibit convective structures beyond the synoptic scale, this work ignores the large-scale organization of convection; it is not consistent, therefore, with the scale separation we found in the size distribution of the regions humidified by convection.

Acknowledgments. It is a pleasure to thank J. D. Neelin and R. Roca for useful advice and comments. This work was supported in part by NSF grant ATM00-82131 to M. Ghil.

References

- Arakawa, A., and W. H. Schubert (1974), Interaction of a cumulus cloud ensemble with the large-scale environment, Part I, *J. Atmos. Sci.*, *31*, 674–701.
- Battisti, D. S., E. S. Sarachik, and A. C. Hirst (1999), A consistent model for the large-scale steady surface atmospheric circulation in the tropics, *J. Clim.*, *12*, 2956–2964.
- Bellon, G., H. Le Treut, and M. Ghil (2003), Large-scale and evaporation-wind feedbacks in a box model of the tropical climate, *Geophys. Res. Lett.*, *30* (22), 2145, doi:10.1029/2003GL017895.
- Cahalan, R. F., and J. H. Joseph (1988), Fractal statistics of cloud fields, *Mon. Wea. Rev.*, *117*, 261–272.
- Gill, A. E. (1980), Some simple solutions for heat-induced tropical circulation, *Q. J. Roy. Meteorol. Soc.*, *106*, 447–462.
- Held, I. M., and B. J. Soden (2000), Water vapor and global warming, *Annu. Rev. Energy Environ.*, *25*, 441–475.
- Larson, K., D. L. Hartmann, and S. A. Klein (1999), The role of clouds, water vapor, circulation, and boundary layer structure in the sensitivity of the tropical climate, *J. Clim.*, *12*, 2359–2374.
- Liebmann, B., and C. Smith (1996), Description of a complete (interpolated) outgoing longwave radiation dataset, *Bull. Amer. Meteorol. Soc.*, *77*, 1275–1277.
- Lindzen, R. S., and S. Nigam (1987), On the role of the sea surface temperature gradients in forcing the low-level winds and convergence in the tropics, *J. Atmos. Sci.*, *44*, 2418–2436.
- Lovejoy, S. (1982), Area-perimeter relation for rain and cloud areas, *Science*, *216*, 185–187.
- Pierrehumbert, R. T. (1995), Thermostats, radiator fins, and the local runaway greenhouse, *J. Atmos. Sci.*, *52*, 1784–1806.
- Rosenfeld, A., and A. C. Kak (1982), *Digital Picture Processing*, 830pp., Academic Press, New York.
- Samet, H. (1989), *Applications of Spatial Data Structures: Computer Graphics, Image Processing and GIS*, 507pp., Addison-Wesley Publishing Company, Boston.
- Simmons, A. J. and J. K. Gibson (2000), *The ERA-40 Project Plan, ERA-40 Project Report Series No. 1*, 63 pp., European Centre for Medium-range Weather Forecast, Reading.
- Stevens, B., J. Duan, J. C. McWilliams, M. Munnich, and J. D. Neelin (2002), Entrainment, Rayleigh friction, and boundary layer winds over the tropical Pacific, *J. Climate*, *15*, 30–44.
- Zhang, C., B. E. Mapes, and B. J. Soden (2003), Bimodality in tropical water vapour, *Q. J. Roy. Meteorol. Soc.*, *129*, 2849–2866.

¹Also at the Department of Atmospheric and Oceanic Sciences, University of California at Los Angeles, Los Angeles, California.